Economic Model Predictive Control of Nonlinear Process Systems Using Lyapunov Techniques

Mohsen Heidarinejad

Dept. of Electrical Engineering, University of California Los Angeles CA 90095

Jinfeng Liu, and Panagiotis D. Christofides

Dept. of Chemical and Biomolecular Engineering, University of California Los Angeles CA 90095

In this work, we develop model predictive control (MPC) designs, which are capable of optimizing closed-loop performance with respect to general economic considerations for a broad class of nonlinear process systems. Specifically, in the proposed designs, the economic MPC optimizes a cost function, which is related directly to desired economic considerations and is not necessarily dependent on a steady-state—unlike conventional MPC designs. First, we consider nonlinear systems with synchronous measurement sampling and uncertain variables. The proposed economic MPC is designed via Lyapunov-based techniques and has two different operation modes. The first operation mode corresponds to the period in which the cost function should be optimized (e.g., normal production period); and in this operation mode, the MPC maintains the closed-loop system state within a predefined stability region and optimizes the cost function to its maximum extent. The second operation mode corresponds to operation in which the system is driven by the economic MPC to an appropriate steady-state. In this operation mode, suitable Lyapunov-based constraints are incorporated in the economic MPC design to guarantee that the closed-loop system state is always bounded in the predefined stability region and is ultimately bounded in a small region containing the origin. Subsequently, we extend the results to nonlinear systems subject to asynchronous and delayed measurements and uncertain variables. Under the assumptions that there exist an upper bound on the interval between two consecutive asynchronous measurements and an upper bound on the maximum measurement delay, an economic MPC design which takes explicitly into account asynchronous and delayed measurements and enforces closed-loop stability is proposed. All the proposed economic MPC designs are illustrated through a chemical process example and their performance and robustness are evaluated through simulations. © 2011 American Institute of Chemical Engineers AIChE J, 58: 855–870, 2012
Keywords: economic model predictive control, nonlinear process systems, synchronous measurements, asynchronous and delayed measurements, uncertain variables

Introduction

Maximizing profit has been and will always be the primary purpose of optimal process operation. Within process control, the economic optimization considerations of a plant

Correspondence concerning this article should be addressed to P. D. Christofides at pdc@seas.ucla.edu.

are usually addressed via a real-time optimization (RTO) system (e.g., Ref. 1 and the references therein). In general, an RTO system includes two different layers: the upper layer that optimizes process operation set-points taking into account economic considerations using steady-state system models, and the lower layer (i.e., process control layer) whose primary objective is to employ feedback control systems to force the process to track the set-points. Model predictive control (MPC) is widely adopted in industry in the process control layer because of its ability to deal with large multivariable constrained control problems and to account for optimization considerations.[2,3] The key idea of a standard MPC is to choose control actions by repeatedly solving an online constrained optimization problem, which aims at minimizing a cost function that involves penalties on the state variables and on the control actions over a finite prediction horizon. Typically, the cost function is in quadratic form including penalties on the deviations of the system state and control inputs from a desired steady-state. Because of the structure of the cost function, the control objective of a standard MPC is to drive the state of the closed-loop system to the desired steady-state. In MPC theory, the quadratic cost function is also widely used as a Lyapunov function to prove closed-loop stability (e.g., Ref. 3). Even though in the standard MPC formulations, certain economic optimization considerations can be taken into account (e.g., optimal use of control action), general economic optimization considerations are usually not addressed. To account for general economic optimization considerations, the quadratic cost function used in standard MPC should be replaced by an economics-based cost function. Moreover, the standard MPC should be reformulated in an appropriate way to guarantee closed-loop stability.

Within process control, there have been several calls for the integration of MPC and economic optimization of processes (e.g., Refs 4–6). In the literature, two-stage MPC structures,[7–10] the so-called LP-MPC and QP-MPC, have been investigated to reduce the difference between the sampling rates of the steady-state optimization performed in the RTO layer and the lower layer linear MPC. There are also attempts to integrate steady-state RTO and linear MPC in a single level.[11,12] In this type of approach, the economic optimization and control problems are solved simultaneously in a single optimization problem and an additional term is added into the MPC cost function to account for the economic considerations. There are also attempts to utilize a dynamic model in the RTO layer, which interacts with lower layer linear MPC (e.g., Ref. 13). This approach uses dynamical models in the RTO and recalculates the optimal set-points for the linear MPC only if economic benefits are possible. Furthermore, there are efforts on the development of MPC accounting for general economic considerations in the cost function.[14–16] In Ref. 14, general ideas of a combined steady-state optimization and linear MPC scheme as well as a case study were reported. In Ref. 15, two economically oriented nonlinear MPC formulations were proposed for cyclic processes and nominal stability of the closed-loop system was established via Lyapunov techniques. In,[16] MPC schemes using an economics-based cost function were proposed and the stability properties were established using a suitable Lyapunov function. The MPC schemes in[16] adopt a terminal constraint which requires that the closed-loop system state settles to a steady-state at the end of each optimal input trajectory calculation (i.e., end of the prediction horizon). Even though a rigorous stability analysis is included in Ref. 16, it is difficult, in general, to characterize, a priori, the set of initial conditions starting from where feasibility and closed-loop stability of the proposed MPC scheme are guaranteed.

In this work, we develop Lyapunov-based economic MPC (LEMPC) designs which are capable of optimizing closed-loop performance with respect to general economic considerations for nonlinear systems. The design of the LEMPC is based on uniting receding horizon control with explicit Lyapunov-based nonlinear controller design techniques and allows for an explicit characterization of the stability region of the closed-loop system; such a characterization may be conservative in certain applications and it may be possible for the LEMPC to achieve closed-loop stability for initial conditions outside of the estimated stability region. In the proposed designs, the LEMPC schemes optimize a cost function which is related directly to certain economic considerations and is not necessarily dependent on a steady-state—unlike conventional MPC designs. First, we consider nonlinear systems with synchronous measurement sampling and uncertain variables. The proposed LEMPC is designed via Lyapunov-based techniques and has two different operation modes. The first operation mode corresponds to the period in which the cost function should be optimized (e.g., normal production period); and in this operation mode, the LEMPC maintains the closed-loop system state within a predefined stability region and optimizes the cost function to its maximum extent. The second operation mode corresponds to operation in which the system is driven by the LEMPC to an appropriate steady-state. In the LEMPC design, suitable Lyapunov-based constraints are incorporated to guarantee that the closed-loop system state is always bounded in the predefined stability region and is ultimately bounded in a small region containing the origin. Subsequently, we extend the results to nonlinear systems subject to asynchronous and delayed measurements and uncertain variables. Under the assumptions that there exist an upper bound on the interval between two consecutive asynchronous measurements and an upper bound on the maximum measurement delay, an LEMPC design which takes explicitly into account asynchronous and delayed measurements and enforces closed-loop stability is proposed. The theoretical results are illustrated through a chemical process example.

Preliminaries

Notation

The operator $|\cdot|$ is used to denote Euclidean norm of a vector, and a continuous function $\alpha: [0,a) \rightarrow [0,\infty)$ is said to belong to class $\mathcal{K}$ if it is strictly increasing and satisfies $\alpha(0) = 0$. The symbol Ω_r is used to denote the set $\Omega_r := \{x \in R^{n_x}: V(x) \leq r\}$ where V is a scalar function, and the operator '/' denotes set subtraction, that is, $A/B := \{x \in R^{n_x}: x \in A, x \notin B\}$. The symbol diag (v) denotes a matrix whose diagonal elements are the elements of vector v and all the other elements are zeros.

Class of nonlinear systems

We consider a class of nonlinear systems which can be described by the following state-space model

$$\dot{x}(t) = f(x(t), u_1(t), \ldots, u_m(t), w(t)) \qquad (1)$$

where $x(t) \in R^{n_x}$ denotes the vector of state variables of the system and $u_i(t) \in R$, $i = 1,\ldots,m$, and $w(t) \in R^{n_w}$ denote m control (manipulated) inputs and the disturbance vector, respectively. The m control inputs are restricted to be in m nonempty convex sets $U_i \subseteq R$, $i = 1,\ldots,m$, which are defined as $U_i := \{u_i \in R: |u_i| \le u_i^{max}\}$ where u_i^{max}, $i = 1,\ldots,m$, are the magnitudes of the input constraints. The disturbance $w(t) \in R^{n_w}$ is bounded, i.e., $w(t) \in W$ where $W := \{w \in R^{n_w} \text{ s.t. } |w| \le \theta, \theta > 0\}$. We assume that f is a locally Lipschitz vector function and that the origin is an equilibrium point of the unforced nominal system (i.e., the system of Eq. 1 with $u_i(t) \equiv 0$, $i = 1,\ldots,m$ and $w(t) \equiv 0$ for all times) which implies that $f(0,0,\ldots,0,0) = 0$.

Lyapunov-based controller

We assume that there exists a Lyapunov-based controller $h(x) = [h_1(x) \cdots h_m(x)]^T$ which renders the origin of the nominal closed-loop system asymptotically stable with $u_i = h_i(x)$, $i = 1,\ldots,m$, while satisfying the input constraints for all the states x inside a given stability region. We note that this assumption is essentially equivalent to the assumption that the system is stabilizable or that the pair (A,B) in the case of linear systems is stabilizable. Using converse Lyapunov theorems,[17,18] this assumption implies that there exist class $\mathcal{K}$ functions $\alpha_i(\cdot), i = 1,2,3,4$ and a continuously differentiable

Lyapunov function $V(x)$ for the nominal closed-loop system that satisfy the following inequalities

$$
\begin{aligned}
\alpha_1(|x|) &\le V(x) \le \alpha_2(|x|) \\
\tfrac{\partial V(x)}{\partial x} f(x, h_1(x), \ldots, h_m(x), 0) &\le -\alpha_3(|x|) \\
\left| \tfrac{\partial V(x)}{\partial x} \right| &\le \alpha_4(|x|) \\
h_i(x) &\in U_i, \ i = 1, \ldots, m
\end{aligned} \qquad (2)
$$

for all $x \in O \subseteq R^{n_x}$ where O is an open neighborhood of the origin. We denote the region $\Omega_\rho \subseteq O$ as the stability region of the closed-loop system under the Lyapunov-based controller $h(x)$. Note that explicit stabilizing control laws that provide explicitly defined regions of attraction for the closed-loop system have been developed using Lyapunov techniques for specific classes of nonlinear systems, particularly input-affine nonlinear systems; the reader may refer to[18–21] for results in this area including results on the design of bounded Lyapunov-based controllers by taking explicitly into account constraints for broad classes of nonlinear systems.

By continuity, the local Lipschitz property assumed for the vector field f and taking into account that the manipulated inputs u_i, $i = 1,\ldots,m$ are bounded, there exists a positive constant M such that

$$|f(x, u_1, \ldots, u_m, w)| \le M \qquad (3)$$

for all $x \in \Omega_\rho$ and $u_i \in U_i$, $i = 1,\ldots,m$. In addition, by the continuous differentiable property of the Lyapunov function $V(x)$ and the Lipschitz property assumed for the vector field f, there exist positive constants L_x, L_w, L_x', and L_w' such that

$$
\begin{aligned}
|f(x, u_1, \ldots, u_m, w) - f(x', u_1, \ldots, u_m, 0)| &\le L_x|x - x'| + L_w|w| \\
\left| \tfrac{\partial V(x)}{\partial x} f(x, u_1, \ldots, u_m, w) - \tfrac{\partial V(x')}{\partial x} f(x', u_1, \ldots, u_m, 0) \right| &\le L_x'|x - x'| + L_w'|w|
\end{aligned} \qquad (4)
$$

for all $x,x' \in \Omega_\rho$, $u_i \in U_i$, $i = 1,\ldots,m$ and $w \in W$.

Remark 1. *We note that while there are currently no general methods for constructing Lyapunov functions for general nonlinear systems, for broad classes of nonlinear systems arising in the context of chemical process control applications, quadratic Lyapunov functions have been widely used and have been demonstrated to yield very good estimates of closed-loop stability regions[18]; please see also "Application to a chemical process example" section.*

Remark 2. *Note that in the present work, we use the level set Ω_ρ of the Lyapunov function $V(x)$ to estimate the stability region (i.e., domain of attraction) of the closed-loop system under the controller $h(x)$. Specifically, an estimate of the domain of attraction of the closed-loop system is computed as follows: first, a controller (e.g., $h(x)$) is designed that makes the time-derivative of a Lyapunov function, $V(x)$, along the closed-loop system trajectory negative definite around the equilibrium point; then, an estimate of the set where $\dot{V}$ is negative is computed, and finally, a level set (ideally the largest) of V (denoted by Ω_ρ in the present work) embedded in the set where $\dot{V}$ is negative, is computed. From this approach to calculate Ω_ρ, we can conclude that the set Ω_ρ is a guaranteed closed-loop stability set but it is possible*

that the controller $h(x)$ stabilizes the closed-loop system for initial conditions outside of the set Ω_ρ.

Lyapunov-Based Economic MPC with Synchronous Measurement Sampling

In this section, we design LEMPC for the system of Eq. 1 with synchronous measurement sampling. We assume that the state x of the system is sampled synchronously and the time instants at which we have state measurements are indicated by the time sequence $\{t_{k \ge 0}\}$ with $t_k = t_0 + k\Delta$, $k = 0,1,\ldots$ where t_0 is the initial time and Δ is the sampling time.

In the proposed design, the LEMPC maximizes a cost function which takes into account specific economic considerations and it has two operation modes. In the first operation mode, the LEMPC optimizes the economic cost function while maintaining the system state within the stability region Ω_ρ (i.e., $x(t) \in \Omega_\rho$); in the second operation mode, the LEMPC drives the state of the system to a desired steady-state. The economic MPC is designed via Lyapunov-based MPC techniques[22] to take advantage of the stability properties of the Lyapunov-based controller $h(x)$. Specifically, we

assume that from the initial time t_0 up to a specific time t', the LEMPC operates in the first operation mode to maximize the economic cost function; after the time t', we assume that the LEMPC operates in the second operation mode and calculates the inputs in a way that the state of the closed-loop system is driven to a neighborhood of the desired steady-state (i.e., the origin $x = 0$). The proposed LEMPC provides more degrees of freedom in the economic optimal operation of the system and can eventually regulate the system state to a desired steady-state. For simplicity and without loss of generality in the rest of this article, we assume that the specific time t' is an integer multiple of the sampling time of the MPC, Δ.

Implementation strategy

From the initial time t_0 to t', the LEMPC operates in the first operation mode. In the design of the LEMPC, one important issue we need to consider is the effect of the bounded disturbance w on the stability of the closed-loop system. To take the disturbance w into account explicitly, we consider a region $\Omega_{\tilde{\rho}}$, $\tilde{\rho}<\rho$. Specifically, when $x(t_k)$ is received at a sampling time t_k, if $x(t_k)$ is in the region $\Omega_{\tilde{\rho}}$, the LEMPC maximizes the cost function within the region $\Omega_{\tilde{\rho}}$; if $x(t_k)$ is in the region $\Omega_{\rho}/\Omega_{\tilde{\rho}}$, the LEMPC first drives the system state to the region $\Omega_{\tilde{\rho}}$ and then maximizes the cost function within $\Omega_{\tilde{\rho}}$. Note that the region $\Omega_{\tilde{\rho}}$ plays the role of a "safe" zone in which the LEMPC can maximize the cost function to its maximum extent while the effect of the disturbance w on the closed-loop stability is taken into account. Note also that the relation between $\tilde{\rho}$ and ρ is determined by the system property (i.e., the properties of the vector function f), the upper bound on the disturbance (i.e., θ) and the sampling time of the LEMPC. This relation will be characterized in Eq. 12 in Theorem 1.

After time t', the system operates in the second operation mode. In this operation mode, the LEMPC calculates the inputs in a way that the Lyapunov function of the system continuously decreases to steer the state of the system to a neighborhood of the origin.

The implementation strategy of the proposed LEMPC with synchronous measurement sampling can be summarized as follows:

1. At a sampling time t_k, the controller receives the system state $x(t_k)$ from the sensors.
2. If $t_k < t'$, go to Step 3. Else, go to Step 4.
3. If $x(t_k) \in \Omega_{\tilde{\rho}}$, go to Step 3.1. Else, go to Step 3.2.
    3.1 The controller maximizes the economic cost function within $\Omega_{\tilde{\rho}}$. Go to Step 5.
    3.2 The controller drives the system state to the region $\Omega_{\tilde{\rho}}$. Go to Step 5.
4. The controller drives the system state to a small neighborhood of the desired steady-state.
5. Go to Step 1 ($k \leftarrow k + 1$).

LEMPC formulation

The optimization problem of the proposed LEMPC for the system of Eq. 1 with synchronous measurement sampling is as follows

$$\max_{u_1,\dots,u_m \in S(\Delta)} \int_{t_k}^{t_{k+N}} L(\tilde{x}(\tau), u_1(\tau), \dots, u_m(\tau))d\tau \quad (5a)$$

$$\text{st. } \dot{\tilde{x}}(t) = f(\tilde{x}(t), u_1(t), \dots, u_m(t), 0) \quad (5b)$$

$$u_i(t) \in U_i, \ i = 1, \dots, m \quad (5c)$$

$$\tilde{x}(t_k) = x(t_k) \quad (5d)$$

$$V(\tilde{x}(t)) \leq \tilde{\rho}, \ \forall t \in [t_k, t_{k+N}], \text{ if } t_k \leq t' \text{ and } V(x(t_k)) \leq \tilde{\rho}$$
$$\frac{\partial V(x(t_k))}{\partial x}f(x(t_k), u_1(t_k), \dots, u_m(t_k), 0) \quad (5e)$$

$$\leq \frac{\partial V(x(t_k))}{\partial x}f(x(t_k), h_1(x(t_k)), \dots, h_m(x(t_k)), 0),$$
$$\text{if } t_k > t' \text{ or } \tilde{\rho} < V(x(t_k)) \leq \rho \quad (5f)$$

where $S(\Delta)$ is the family of piece-wise constant functions with sampling period Δ, N is the prediction horizon of this LEMPC, $L(\tilde{x}(\tau), u_1(\tau), \dots, u_m(\tau))$ is the economic measure which defines the cost function, the state $\tilde{x}$ is the predicted trajectory of the system with $u_1,\dots,u_m$ computed by the LEMPC and $x(t_k)$ is the state measurement obtained at time t_k. The optimal solution to this optimization problem is denoted by $u_i^*(t|t_k)$, $i = 1,\dots,m$, which is defined for $t \in [t_k, t_{k+N}]$.

In the optimization problem of Eq. 5, the constraint of Eqs. 5b is the nominal model of the system of Eq. 1 (i.e., $w(t) = 0$ for all t) and is used to predict the future evolution of the closed-loop system; the constraint of Eq. 5c defines the input constraints on all the inputs; the constraint of Eq. 5d defines the initial condition of the optimization problem; the constraint of Eq. 5e is only active when $x(t_k) \in \Omega_{\tilde{\rho}}$ in the first operation mode and is incorporated to ensure that the predicted state evolution of the closed-loop system is maintained in the region $\Omega_{\tilde{\rho}}$ (thus, the actual state of the closed-loop system is in the stability region Ω_{ρ}); the constraint of Eq. 5f is only active in the second operation mode or when $\tilde{\rho} < V(x(t_k)) \leq \rho$ in the first operation mode. This constraint is used to enforce that the Lyapunov function of the system decreases at least at the rate given by the Lyapunov-based controller $h(x)$ implemented in a sample-and-hold fashion.

The manipulated inputs of the proposed control design from time t_k to t_{k+1} ($k = 0,1,2,\dots$) are defined as follows

$$u_i(t) = u_i^*(t|t_k), \ i = 1, \dots, m, \ \forall t \in [t_k, t_{k+1}) \quad (6)$$

Stability analysis

In this subsection, we present the stability properties of the proposed LEMPC of Eq. 5 for the system of Eq. 1 with synchronous measurement sampling. To proceed, we need the following two propositions.

Proposition 1 (c.f. Ref. 23). *Consider the systems*

$$\dot{x}_a(t) = f(x_a(t), u_1(t), \dots, u_m(t), w(t))$$
$$\dot{x}_b(t) = f(x_b(t), u_1(t), \dots, u_m(t), 0) \quad (7)$$

with initial states $x_a(t_0) = x_b(t_0) \in \Omega_{\rho}$. *There exists a* $\mathcal{K}$ *function* $f_W(\cdot)$ *such that*

$$|x_a(t) - x_b(t)| \leq f_W(t - t_0), \quad (8)$$

for all $x_a(t), x_b(t) \in \Omega_\rho$ *and all* $w(t) \in W$ *with*

$$f_W(\tau) = \frac{L_w \theta}{L_x}(e^{L_x \tau} - 1) \quad (9)$$

Proposition 1 provides an upper bound on the deviation of the state trajectory obtained using the nominal model, from the actual system state trajectory when the same control input trajectories are applied. Proposition 2 below bounds the difference between the magnitudes of the Lyapunov function of two different states in Ω_ρ.

Proposition 2. (c.f. Ref. 23). *Consider the Lyapunov function* $V(\cdot)$ *of the system of* Eq. 1. *There exists a quadratic function* $f_V(\cdot)$ *such that*

$$V(x) \leq V(\hat{x}) + f_V(|x - \hat{x}|) \quad (10)$$

for all $x, \hat{x} \in \Omega_\rho$ *with*

$$f_V(s) = \alpha_4(\alpha_1^{-1}(\rho))s + M_v s^2 \quad (11)$$

where M_v *is a positive constant.*

Theorem 1 below provides sufficient conditions under which the LEMPC of Eq. 5 guarantees that the state of the closed-loop system of Eq. 1 is always bounded in Ω_ρ and is ultimately bounded in a small region containing the origin.

Theorem 1. *Consider the system of* Eq. 1 *in closed-loop under the LEMPC design of* Eq. 5 *based on a controller* $h(x)$ *that satisfies the conditions of* Eq. 2. *Let* $\varepsilon_w > 0$, $\Delta > 0$, $\rho > \tilde{\rho} > 0$ *and* $\rho > \rho_s > 0$ *satisfy*

$$\tilde{\rho} \leq \rho - f_V(f_W(\Delta)) \quad (12)$$

and

$$-\alpha_3(\alpha_2^{-1}(\rho_s)) + L_x' M\Delta + L_w'\theta \leq -\varepsilon_w/\Delta \quad (13)$$

If $x(t_0) \in \Omega_\rho$, $\rho_s \leq \tilde{\rho}$, $\rho_{\min} \leq \rho$ *and* $N \geq 1$ *where*

$$\rho_{\min} = \max\{V(x(t + \Delta)) : V(x(t)) \leq \rho_s\} \quad (14)$$

then the state $x(t)$ *of the closed-loop system is always bounded in* Ω_ρ *and is ultimately bounded in* $\Omega_{\rho_{\min}}$.

Proof. The proof consists of three parts. We first prove that the optimization problem of Eq. 5 is feasible for all states $x \in \Omega_\rho$. Subsequently, we prove that, in the first operation mode, under the LEMPC design of Eq. 5, the closed-loop state of the system of Eq. 1 is always bounded in Ω_ρ. Finally, we prove that, in the second operation mode, under the LEMPC of Eq. 5, the closed-loop state of the system of Eq. 1 is ultimately bounded in $\rho_{\min}$.

Part 1: When $x(t)$ is maintained in Ω_ρ (which will be proved in Part 2), the feasibility of the LEMPC of Eq. 5 follows because input trajectories $u_i(t)$, $i = 1,...,m$, such that $u_i(t) = h_i(x(t_{k+j}))$, $\forall t \in [t_{k+j}, t_{k+j+1})$ with $j = 0,..., N - 1$ are feasible solutions to the optimization problem of Eq. 5 since such trajectories satisfy the input constraint of Eq. 5c and the Lyapunov-based constraints of Eqs. 5e and 5f. This is guaranteed by the closed-loop stability property of the Lyapunov-based controller $h(x)$; the reader may refer to[24] for more detailed discussion on the stability property of the Lyapunov-based controller $h(x)$.

Part 2: We assume that the LEMPC of Eq. 5 operates in the first operation mode. We prove that if $x(t_k) \in \Omega_{\tilde{\rho}}$, then $x(t_{k+1}) \in \Omega_\rho$; and if $x(t_k) \in \Omega_\rho/\Omega_{\tilde{\rho}}$, then $V(x(t_{k+1})) < V(x(t_k))$ and in finite steps, the state converges to $\Omega_{\tilde{\rho}}$ (i.e., $x(t_{k+j}) \in \Omega_{\tilde{\rho}}$ where j is a finite positive integer).

When $x(t_k) \in \Omega_{\tilde{\rho}}$, from the constraint of Eq. 5e, we obtain that $\tilde{x}(t_{k+1}) \in \Omega_{\tilde{\rho}}$. By Propositions 1 and 2, we have that

$$V(x(t_{k+1})) \leq V(\tilde{x}(t_{k+1})) + f_V(f_W(\Delta)) \quad (15)$$

Since $V(\tilde{x}(t_{k+1})) \leq \tilde{\rho}$, if the condition of Eq. 12 is satisfied, we can conclude that

$$x(t_{k+1}) \in \Omega_\rho$$

when $x(t_k) \in \Omega_\rho/\Omega_{\tilde{\rho}}$, from the constraint of Eq. 5f and the condition of Eq. 2, we can write

$$\frac{\partial V(x(t_k))}{\partial x}f(x(t_k), u_1^*(t_k), ..., u_m^*(t_k), 0)$$
$$\leq \frac{\partial V(x(t_k))}{\partial x}f(x(t_k), h_1(x(t_k)), ..., h_m(x(t_k)), 0) \leq -\alpha_3(|x(t_k)|)$$
$$(16)$$

The time derivative of the Lyapunov function along the computed optimal trajectories $u_1^*,...,u_m^*$ for $\forall \tau \in [t_k, t_{k+1})$ can be written as follows

$$\dot{V}(x(\tau)) = \frac{\partial V(x(\tau))}{\partial x}f(x(\tau), u_1^*(t_k), ..., u_m^*(t_k), w(\tau)) \quad (17)$$

Adding and subtracting the term $\frac{\partial V(x(t_k))}{\partial x}f(x(t_k), u_1^*(t_k), ..., u_m^*(t_k), 0)$ to/from the above equation and considering Eq. 16, we have

$$\dot{V}(x(\tau)) \leq -\alpha_3(|x(t_k)|) + \frac{\partial V(x(\tau))}{\partial x}f(x(\tau), u_1^*(t_k), ..., u_m^*(t_k), w(\tau))$$
$$- \frac{\partial V(x(t_k))}{\partial x}f(x(t_k), u_1^*(t_k), ..., u_m^*(t_k), 0) \quad (18)$$

Due to the fact that the disturbance is bounded $|w| \leq \theta$ and the Lipschitz properties of Eq. 4, we can write

$$\dot{V}(x(\tau)) \leq -\alpha_3(|x(t_k)|) + L_x'|x(\tau) - x(t_k)| + L_w'\theta \quad (19)$$

Taking into account Eq. 3 and the continuity of $x(t)$, the following bound can be written for all $\tau \in [t_k, t_{k+1})$

$$|x(\tau) - x(t_k)| \leq M\Delta \quad (20)$$

Since $x(t_k) \in \Omega_\rho/\Omega_{\tilde{\rho}}$, it can be concluded that $x(t_k) \in \Omega_\rho/\Omega_{\rho_s}$. Thus, we can write

$$\dot{V}(x(\tau)) \leq -\alpha_3(\alpha_2^{-1}(\rho_s)) + L_x'M\Delta + L_w'\theta \quad (21)$$

If the condition of Eq. 13 is satisfied, then there exists $\varepsilon_w > 0$ such that the following inequality holds for $x(t_k) \in \Omega_\rho/\Omega_{\tilde{\rho}}$

$$\dot{V}(x(t)) \leq -\varepsilon_w/\Delta, \ \forall t = [t_k, t_{k+1})$$

Integrating this bound on $t \in [t_k, t_{k+1})$, we obtain that

$$V(x(t_{k+1})) \leq V(x(t_k)) - \varepsilon_w$$

$$V(x(t)) \leq V(x(t_k)), \ \forall t \in [t_k, t_{k+1}) \qquad (22)$$

for all $x(t_k) \in \Omega_\rho/\Omega_{\tilde{\rho}}$. Using Eq. 22 recursively, it is proved that, if $x(t_k) \in \Omega_\rho/\Omega_{\tilde{\rho}}$, the state converges to $\Omega_{\tilde{\rho}}$ in a finite number of sampling times without leaving the stability region.

Part 3: We assume that the LEMPC of Eq. 5 operates in the second operation mode. We prove that if $x(t_k) \in \Omega_\rho$, then $V(x(t_{k+1})) \leq V(x(t_k))$ and the system state is ultimately bounded in an invariant set $\Omega_{\rho_{\min}}$. Following similar steps as in Part 2, we can derive that the inequality of Eq. 22 hold for all $x(t_k) \in \Omega_\rho/\Omega_{\rho_s}$. Using this result recursively, it is proved that, if $x(t_k) \in \Omega_\rho/\Omega_{\rho_s}$, the state converges to Ω_{ρ_s} in a finite number of sampling times without leaving the stability region. Once the state converges to $\Omega_{\rho_s} \subseteq \Omega_{\rho_{\min}}$, it remains inside $\Omega_{\rho_{\min}}$ for all times. This statement holds because of the definition of $\rho_{\min}$. This proves that the closed-loop system state under the LEMPC of Eq. 5 is ultimately bounded in $\Omega_{\rho_{\min}}$. ∎

Remark 3. *Note that the set Ω_ρ (i.e., $V \leq \rho$) is an invariant set for the nominal closed-loop system and is also an invariant set for the closed-loop system subject to bounded disturbances w (i.e., $|w| \leq \theta$) under piece-wise continuous control action implementation when the conditions stated in Theorem 1 (as well as Theorem 2 presented in the next section) are satisfied. This can be interpreted as follows: $\dot{V}$ is negative everywhere in Ω_ρ but the origin when there are no disturbances and the control actions are updated continuously; furthermore, the further away from the origin the more negative $\dot{V}$ is. This implies that for sufficiently small disturbances (i.e., θ sufficiently small) and sufficiently small sampling time (i.e., Δ sufficiently small) $\dot{V}$ of the uncertain closed-loop system will continue to be negative for all $x \in \Omega_\rho$ but in a small ball around the origin (i.e., $\Omega_{\rho_{\min}}$).*

Remark 4. *Note that the term "ultimately bounded" for the state of a nonlinear dynamic system (particularly of the closed-loop system in the present work) means that after a sufficiently large time, t_q, the state of the closed-loop system enters a compact (closed and bounded) set including the origin (i.e., $\Omega_{\rho_{\min}}$ for the closed-loop system of Eq. 1 under the LEMPC of Eq. 5) and stays within this set for all times $t \geq t_q$ (i.e., $x(t) \in \Omega_{\rho_{\min}}$ for $t \geq t_q$).*

Remark 5. *Instead of requiring that the closed-loop system state settles to a steady-state at the end of the prediction horizon as in,[16] in the proposed design, the LEMPC of Eq. 5 has two different operation modes. In the first operation mode, the LEMPC optimizes the economic cost function within the region $\Omega_{\tilde{\rho}}$. When the proposed LEMPC is in the second operation mode, it drives the closed-loop system state to the steady-state. The LEMPC of Eq. 5 also possesses a stability region which can be explicitly characterized.*

Remark 6. *Note that to achieve optimal performance, in general, the prediction horizon of the LEMPC of Eq. 5 should be long enough to cover the period in which the process operation should be optimized. However, long prediction horizon may not be practical for a real-time implementation of an MPC algorithm (especially when nonlinear systems with a large number of manipulated inputs are considered) because of the high computational burden. For certain applications, we may overcome this issue by driving*

part of the system states to certain economic optimal setpoints and operating the rest of the system states in a time-varying manner to further maximize the economic cost function. This implies that we operate part of the system in the second operation mode and part of the system in the first operation mode simultaneously. Please see the example section for an application of this approach to a chemical process example.

Lyapunov-Based Economic MPC with Asynchronous and Delayed Measurements

In this section, we consider the design of LEMPC for systems subject to asynchronous and delayed measurements. Specifically, we assume that the state of the system of Eq. 1, $x(t)$, is available at asynchronous time instants $\{t_{a \geq 0}\}$ which is a random increasing sequence and the interval between two consecutive time instants is not fixed. We also assume that there are delays involved in the measurements. To model delays in measurements, an auxiliary variable d_a is introduced to indicate the delay corresponding to the measurement received at time t_a, that is, at time t_a, the measurement $x(t_a - d_a)$ is received. To study the stability properties in a deterministic framework, we assume that there exists an upper bound T_m on the interval between two successive measurements (i.e., $\max_a\{t_{a+1} - t_a\} \leq T_m$ and an upper bound D on the delays (i.e., $d_a \leq D$). These assumptions are reasonable from a process control perspective. Because the delays are time-varying, it is possible that at a time instant t_a, the controllers may receive a measurement $x(t_a - d_a)$ which does not provide new information (i.e., $t_a - d_a < t_{a-1} - d_{a-1}$) and the maximum amount of time the system might operate in open-loop following t_a is $D + T_m - d_a$. This upper bound will be used in the formulation of LEMPC for systems subject to asynchronous and delayed measurements. The reader may refer to[25] for more discussion on the modeling of asynchronous and delayed measurements.

LEMPC implementation strategy

At each asynchronous sampling time, when a delayed measurement is received, we propose to take advantage of the nominal system model of Eq. 1 and the manipulated inputs that have been applied to the system to estimate the current system state from the delayed measurement. Based on the estimate of the current system state, an MPC optimization problem is solved to decide the optimal future input trajectory that will be applied until the next new measurement is received. Similar to previous section, we introduce an LEMPC design which maximizes a cost function accounting for specific economic considerations. This LEMPC also has two operation modes.

From the initial time t_0 to t', the LEMPC operates in the first operation mode. In this operation mode, the proposed LEMPC maximizes an economics-based cost function while maintaining the closed-loop system state in the stability region Ω_ρ. To account for the asynchronous and delayed measurement as well as the disturbance, we consider another region $\Omega_{\hat{\rho}}$ with $\hat{\rho} < \rho$. Specifically, when a delayed measurement is received at a sampling time, the current system state is estimated. If the estimated current state is in the

region $\Omega_{\hat{\rho}}$, the LEMPC maximizes the cost function within the region $\Omega_{\hat{\rho}}$; if the estimated current state is in the region $\Omega_{\rho}/\Omega_{\hat{\rho}}$, the LEMPC first drives the system state to the region $\Omega_{\hat{\rho}}$ and then maximizes the cost function within $\Omega_{\hat{\rho}}$. The relation between ρ and $\hat{\rho}$ will be characterized in Eq. 29 in Theorem 2.

After time t', the system operates in the second operation mode. In this operation mode, the LEMPC calculates the inputs in a way that the Lyapunov function of the system continuously decreases to steer the state of the system to a neighborhood of the origin while taking into account asynchronous and delayed measurements.

The implementation strategy of the proposed LEMPC for systems subject to asynchronous and delayed measurements can be summarized as follows:

1. At a sampling time t_a, the controller receives the system state $x(t_a - d_a)$ from the sensors and estimates the current system state, $\check{x}(t_a)$
2. If $t_a < t'$, go to Step 3. Else, go to Step 4.
3. If $\check{x}(t_a) \in \Omega_{\hat{\rho}}$, go to Step 3.1. Else, go to Step 3.2.
   3.1 The controller maximizes the economic cost function within $\Omega_{\hat{\rho}}$. Go to Step 5.
   3.2 The controller drives the system state to the region $\Omega_{\hat{\rho}}$. Go to Step 5.
4. The controller drives the system state to a small neighborhood of the origin.
5. Go to Step 1 ($a \leftarrow a + 1$).

LEMPC formulation

At a sampling time t_a, the MPC is evaluated to obtain the future input trajectories based on the received system state value $x(t_a - d_a)$. Specifically, the optimization problem of the proposed LEMPC for systems subject to asynchronous and delayed measurements at t_a is as follows

$$\max_{u_1,\dots,u_m \in S(\Delta)} \int_{t_a}^{t_a+N\Delta} L(\check{x}(\tau), u_1(\tau), \dots, u_m(\tau)) d\tau \qquad (23a)$$

$$\text{s.t. } \dot{\check{x}}(t) = f(\check{x}(t), u_1(t), \dots, u_m(t), 0) \qquad (23b)$$

$$u_i(t) = u_i^*(t), \ i = 1, \dots, m, \ t \in [t_a - d_a, t_a) \qquad (23c)$$

$$u_i(t) \in U_i, \ i = 1, \dots, m, \ t \in [t_a, t_a + N\Delta) \qquad (23d)$$

$$\check{x}(t_a - d_a) = x(t_a - d_a) \qquad (23e)$$

$$\dot{\hat{x}}(t) = f(\hat{x}(t), h_1(\hat{x}(t_a + l\Delta)), \dots, h_m(\hat{x}(t_a + l\Delta)), 0)$$
$$\forall t \in [t_a + l\Delta, t_a + (l+1)\Delta), \ l = 0, \dots, N-1 \qquad (23f)$$

$$\hat{x}(t_a) = \check{x}(t_a) \qquad (23g)$$

$$V(\check{x}(t)) \le \hat{\rho}, \ \forall t \in [t_a, t_a + N\Delta), \ \text{if } t_a \le t' \text{ and } V(\check{x}(t_k)) \le \hat{\rho} \qquad (23h)$$

$$V(\check{x}(t)) \le V(\hat{x}(t)), \ \forall t \in [t_a, t_a + N_{Da}\Delta),$$
$$\text{if } t_a > t' \text{ or } \hat{\rho} < V(\check{x}(t_a)) \le \rho \qquad (23i)$$

where $\check{x}$ is the predicted trajectory of the system with control inputs calculated by this LEMPC, $u_i^*(t)$ with $i = 1,\dots,m$ denotes the actual inputs that have been applied to the system,

$x(t_a - d_a)$ is the received delayed measurement, $\hat{x}$ is the predicted trajectory of the system with the control inputs determined by $h(x)$ implemented in a sample-and-hold fashion, and N_{Da} is the smallest integer that satisfies $T_m + D - d_a \le N_{Da}\Delta$. The optimal solution to this optimization problem is denoted by $u_i^{a,*}(t|t_a)$, $i = 1,\dots,m$, which is defined for $t \in [t_a, t_a + N\Delta)$.

There are two types of calculations in the optimization problem of Eq. 23. The first type of calculation is to estimate the current state $\check{x}(t_a)$ based on the delayed measurement $x(t_a - d_a)$ and input values have been applied to the system from $t_a - d_a$ to t_a (constraints of Eqs. 23b, c, and e). The second type of calculation is to evaluate the optimal input trajectory of u_i ($i = 1,\dots,m$) based on $\check{x}(t_a)$ while satisfying the input constraint of Eq. 23d and the stability constraints of Eqs. 23h, i. Note that the length of the constraint N_{Da} depends on the current delay d_a, and thus, it may have different values at different time instants and has to be updated before solving the optimization problem of Eq. 23.

The manipulated inputs of the LEMPC of Eq. 23 for systems subject to asynchronous and delayed measurements are defined as follows

$$u_j(t) = u_j^{a,*}(t|t_a), \ \forall t \in [t_a, t_{a+i}) \qquad (24)$$

for all t_a such that $t_a - d_a > \max_{1<a} t_l - d_l$ and for a given t_a, the variable i denotes the smallest integer that satisfies $t_{a+i} - d_{a+i} > t_a - d_a$ and $j = 1,\dots,m$.

Stability analysis

In this subsection, we present the stability properties of the proposed LEMPC of Eq. 23 in the presence of asynchronous and delayed measurements. To proceed, we need the following proposition.

Proposition 3 (c.f. Refs. 23 and 24). *Consider the nominal sampled trajectory $\hat{x}(t)$ of the system of* Eq. 1 *in closed-loop for a controller $h(x)$, which satisfies the condition of* Eq. 2, *obtained by solving recursively*

$$\dot{\hat{x}}(t) = f(\hat{x}(t), h_1(\hat{x}(t_k)), \dots, h_m(\hat{x}(t_k)), 0), \ t \in [t_k, t_{k+1}) \quad (25)$$

where $t_k = t_0 + k\Delta$, $k = 0,1,\dots$. Let $\Delta, \varepsilon_s > 0$ and $\rho > \rho_s > 0$ satisfy

$$-\alpha_3(\alpha_2^{-1}(\rho_s)) + L_x' M\Delta \le -\varepsilon_s/\Delta \qquad (26)$$

Then, if $\hat{x}(t_0) \in \Omega_{\rho}$ and $\rho_{\min} < \rho$ where $\rho_{\min}$ is defined in Eq. 14, *the following inequality holds*

$$V(\hat{x}(t)) \le V(\hat{x}(t_k)), \ \forall t \in [t_k, t_{k+1}) \qquad (27)$$

$$V(\hat{x}(t_k)) \le \max\{V(\hat{x}(t_0)) - k\varepsilon_s, \rho_{\min}\} \qquad (28)$$

Proposition 3 ensures that if the nominal system controlled by the Lyapunov-based controller $h(x)$ implemented in a sample-and-hold fashion and with open-loop state estimation starts in Ω_{ρ}, then it is ultimately bounded in $\Omega_{\rho_{\min}}$. Theorem 2 below provides sufficient conditions under which the LEMPC of Eq. 23 guarantees that the closed-loop system

state is always bounded in Ω_ρ and is ultimately bounded in a small region containing the origin.

Theorem 2. *Consider the system of Eq. 1 in closed-loop under the LEMPC design of Eq. 23 based on a controller $h(x)$ that satisfies the condition of Eq. 2. Let $\varepsilon_s > 0$, $\Delta > 0$, $\rho > \hat{\rho} > 0$ and $\rho > \rho_s > 0$ satisfy the condition of Eq. 26 and satisfy*

$$\hat{\rho} \leq \rho - f_V(f_W(N\Delta)) \tag{29}$$

and

$$-N_R\varepsilon_s + f_V(f_W(N_D\Delta)) + f_V(f_W(D)) < 0 \tag{30}$$

where N_D is the smallest integer satisfying $N_D\Delta \geq T_m + D$ and N_R is the smallest integer satisfying $N_R\Delta \geq T_m$. If $N \geq N_D$, $\hat{\rho} \geq \rho_s$, $x(t_0) \in \Omega_\rho$, $d_0 = 0$, then the closed-loop state $x(t)$ of the system of Eq. 1 is always bounded in Ω_ρ and is ultimately bounded in $\Omega_{\rho_a} \subset \Omega_\rho$ where

$$\rho_a = \rho_{\min} + f_V(f_W(N_D\Delta)) + f_V(f_W(D)) \tag{31}$$

Proof. When $x(t)$ is maintained in the stability region Ω_ρ, the feasibility of the optimization problem of Eq. 23 can be proved following the same arguments as in Part 1 of the proof of Theorem 1. In the remainder of this proof, we focus on proving that $x(t)$ is always bounded in Ω_ρ and is ultimately bounded in Ω_{ρ_a}. The proof consists of two parts. In Part 1, we prove that $x(t)$ is always maintained in Ω_ρ in the first operation mode; and in Part 2, we prove that $x(t)$ is ultimately bounded in Ω_{ρ_a} in the second operation mode.

In this proof, we assume that $x(t_a - d_a)$ is received at t_a and the next asynchronous measurement containing new information is received at t_{a+i} with $t_{a+i} = t_a + T_m$ and $T_m = N\Delta$. This corresponds to the worst case scenario from feedback control point of view. When $x(t)$ is proved to be bounded in Ω_ρ and ultimately bounded in Ω_{ρ_a} for this worst case, the results are also guaranteed for the general case (i.e., $t_{a+i} \leq t_a + N\Delta$).

Part 1: We assume that the LEMPC of Eq. 23 operates in the first operation mode. We prove that if $\check{x}(t_a) \in \Omega_{\hat{\rho}}$, then $x(t_{a+i}) \in \Omega_\rho$; and if $\check{x}(t_a) \in \Omega_\rho/\Omega_{\hat{\rho}}$, then $V(x(t_{a+i})) < V(x(t_a))$ and in finite steps, the state converges to $\Omega_{\hat{\rho}}$.

When $\check{x}(t_a) \in \Omega_{\hat{\rho}}$, from the constraint of Eq. 23h, we obtain that $\check{x}(t_{a+i}) \in \Omega_{\hat{\rho}}$. When $x(t) \in \Omega_\rho$ for all times (this point will be proved below), we can apply Propositions 1 and 2 to obtain the following inequality

$$V(x(t_{a+i})) \leq V(\check{x}(t_{a+i})) + f_V(f_W(N\Delta)) \tag{32}$$

Since $V(\check{x}(t_{a+i})) \leq \hat{\rho}$, if the condition of Eq. 29 is satisfied, we can conclude that

$$x(t_{a+i}) \in \Omega_\rho \tag{33}$$

when $\check{x}(t_a) \in \Omega_\rho/\Omega_{\hat{\rho}}$, from the condition of Eq. 23i, we can obtain that

$$V(\check{x}(t)) \leq V(\hat{x}(t)), \forall t \in [t_a, t_a + N_{Da}\Delta] \tag{34}$$

By Proposition 3 and taking into account that $\hat{\rho} > \rho_s$, the following inequality can be obtained

$$V(\hat{x}(t_{a+i})) \leq \max\{V(\hat{x}(t_a)) - N_{Da}\varepsilon_s, \rho_{\min}\} \tag{35}$$

By Propositions 1 and 2, we can obtain the following inequalities

$$V(\check{x}(t_a)) \leq V(x(t_a)) + f_V(f_W(d_a)) \tag{36}$$

From the inequalities of Eqs. 32, 35, and 36, we can write that

$$V(x(t_{a+i})) \leq \max\{V(x(t_a)) - N_{Da}\varepsilon_s, \rho_{\min}\} \\ + f_V(f_W(d_a)) + f_V(f_W(N_D\Delta)) \tag{37}$$

Note that in the derivation of the inequality of Eq. 37, we have taken into account that $N_D\Delta \geq T_m + D - d_a$ for all d_a.

To prove that the Lyapunov function is decreasing between t_a and t_{a+i}, the following inequality must hold

$$N_{Da}\varepsilon_s > f_V(f_W(N_D\Delta)) + f_V(f_W(d_a)) \tag{38}$$

for all possible $d_a \leq D$. Taking into account that $f_W(\cdot)$ and $f_V(\cdot)$ are strictly increasing functions of their arguments, that N_{Da} is a decreasing function of the delay d_a and that if $d_a = D$ then $N_{Da} = N_R$, if the condition of Eq. 30 is satisfied, then the condition of Eq. 38 holds for all possible d_a and there exist $\varepsilon_w > 0$ such that the following inequality holds

$$V(x(t_{a+i})) \leq \max\{V(x(t_a)) - \varepsilon_w, \rho_a\} \tag{39}$$

which implies that if $x(t_a) \in \Omega_\rho/\Omega_{\hat{\rho}}$, then $V(x(t_{a+i})) < V(x(t_a))$. This also implies that the state converges to $\Omega_{\hat{\rho}}$ in a finite number of sampling times without leaving the stability region.

Part 2: We assume that the LEMPC of Eq. 23 operates in the second operation mode. We prove that $x(t)$ is ultimately bounded in Ω_{ρ_a}. Following similar steps as in Part 1, we can again derive the condition of Eq. 39. Using this condition recursively, it it proved that, if $x(t_0) \in \Omega_\rho$, then the closed-loop trajectory of the system of Eq. 1 under the LEMPC of Eq. 23 stay in Ω_ρ and satisfy that

$$\limsup_{t \to \infty} V(x(t)) \leq \rho_a \tag{40}$$

This proves the results stated in Theorem 2. ∎

Application to a Chemical Process Example

Consider a well-mixed, non-isothermal continuous stirred tank reactor (CSTR) where an irreversible second-order exothermic reaction $A \rightarrow B$ takes place.[5] A is the reactant and B is the product. The feed to the reactor consists of pure A at flow rate F, temperature T_0 and molar concentration C_{A0}. Due to the nonisothermal nature of the reactor, a jacket is used to remove/provide heat to the reactor. The dynamic equations describing the behavior of the system, obtained through material and energy balances under standard modeling assumptions, are given below:

$$\frac{dC_A}{dt} = \frac{F}{V}(C_{A0} - C_A) - k_0 e^{\frac{-E}{RT}} C_A^2 \tag{41a}$$

$$\frac{dT}{dt} = \frac{F}{V}(T_0 - T) + \frac{-\Delta H}{\sigma C_p} k_0 e^{\frac{-E}{RT}} C_A^2 + \frac{Q}{\sigma C_p V} \tag{41b}$$

where C_A denotes the concentration of the reactant A, T denotes the temperature of the reactor, Q denotes the rate of heat input/removal, V represents the volume of the reactor, ΔH, k_0, and E denote the enthalpy, pre-exponential constant and activation energy of the reaction, respectively and C_p and σ denote the heat capacity and the density of the fluid in the reactor, respectively. The values of the process parameters used in the simulations are shown in Table 1. The process model of Eq. 41 is numerically simulated using an explicit Euler integration method with integration step $h_c = 10^{-4}$ hr.

The process model has one unstable steady state and one stable steady state in the operating range of interest. The control objective is to regulate the process in a region around the unstable steady-state (C_{As}, T_s) to maximize the production rate of B. There are two manipulated inputs. One of the inputs is the concentration of A in the inlet to the reactor, C_{A0}, and the other manipulated input is the external heat input/removal, Q. The steady-state input values associated with the steady-state are denoted by C_{A0s} and Q_s, respectively.

The process model of Eq. 41 belongs to the following class of nonlinear systems

$$\dot{x}(t) = f(x(t)) + g_1(x(t))u_1(t) + g_2(x(t))u_2(t) + w(t)$$

where $x^T = [C_A - C_{As}\ T - T_s]$ is the state, $u_1 = C_{A0} - C_{A0s}$ and $u_2 = Q - Q_s$ are the inputs, $f = [f_1\ f_2]^T$ and $g_i = [g_{i1}\ g_{i2}]^T$ ($i = 1,2$) are vector functions. The inputs are subject to constraints as follows: $|u_1| \leq 3.5$ kmol/m^3 and $|u_2| \leq 5 \times 10^5$ KJ/hr. $w = [w_1\ w_2]^T$ is the bounded disturbance vector (Gaussian white noise with variances $\sigma_1 = 1$ kmol/m^3 and $\sigma_2 = 40\ K$) with $|w_1| \leq 1$ kmol/m^3 and $|w_2| \leq 40\ K$.

The economic measure that we consider in this example is as follows[5].

$$L(x, u_1, u_2) = \frac{1}{t_f} \int_0^{t_f} k_0 e^{-\frac{E}{RT(\tau)}} C_A^2(\tau) d\tau \tag{42}$$

where $t_f = 1$ hr is the final time of the simulation. This economic objective function is to maximize the average production rate over process operation for $t_f = 1$ hr. We also consider that there is limitation on the amount of material which can be used over the period t_f. Specifically, the control input trajectory of u_1 should satisfy the following constraint

$$\frac{1}{t_f} \int_0^{t_f} u_1(\tau) d\tau = 1\ \text{kmol/m}^3 \tag{43}$$

This constraint means that the average amount of u_1 during one period is fixed. For the sake of simplicity and without loss of generality, we will refer to Eq. 43 as the integral constraint. It has been clarified in[5] (see also Refs. 26–29) that by periodic operation through switching between upper and lower bound the average production rate can be improved owing to the second-order dependence of the reac-

Table 1. Parameter Values

$T_0 = 300$	K	$F = 5$	$\frac{m^3}{hr}$
$V = 1.0$	m^3	$E = 5 \times 10^4$	$\frac{kJ}{kmol}$
$k_0 = 8.46 \times 10^6$	$\frac{1}{hr}$	$\Delta H = -1.15 \times 10^4$	$\frac{kJ}{kmol}$
$C_p = 0.231$	$\frac{kJ}{kgK}$	$R = 8.314$	$\frac{kJ}{kmolK}$
$\sigma = 1000$	$\frac{kg}{m^3}$	$C_{As} = 2$	$\frac{kmol}{m^3}$
$T_s = 400$	K	$C_{A0s} = 4$	$\frac{kmol}{m^3}$
$Q_s = 0$	$\frac{KJ}{hr}$		

tion rate on reactant concentration. In other words, since the amount of reactant material over one period of operation is fixed and the reaction is of second-order, to get the maximum reaction rate over one period, all of the material should be fed at the beginning of the process operation period. Since this policy is not practically implementable given the presence of constraints on C_{A0} value, periodic operation is the best practical choice to maximize the average production rate over one period subject to input constraints; please see simulations below.

In the first set of simulations, we assume that the state feedback information is available at synchronous time instants while in the second set of simulations we assume that the controller receives asynchronous and delayed measurements.

Synchronous measurement sampling

We will design an LEMPC following Eq. 5 to manipulate the two control inputs. We assume that the full system state x is measured and sent to the LEMPC at synchronous time instants $t_k = k\Delta$, $k = 0,1,\ldots$, with $\Delta = 0.01$ hr $= 36$ sec. The LEMPC horizon is $N = 10$. For the computation of the stability region, we consider a quadratic Lyapunov function $V(x) = x^T P x$ with $P = $ diag ([716.83 1]). To estimate the stability region Ω_ρ, we evaluate $\dot{V}$ by assuming that u_1 is equally distributed over t_f (i.e., $u_1(\tau) = 1$, $0 \leq \tau \leq t_f$) and utilize feedback linearization for u_2 subject to input constraint $u_2^{\max}$ and bounded disturbance ($|w_1| \leq 1$ kmol/m^3 and $|w_2| \leq 40\ K$).

Since the LEMPC is evaluated at discrete-time instants during the closed-loop simulation, the integral constraint is enforced as follows

$$\sum_{i=0}^{M-1} u_1(t_i) = \frac{t_f}{\Delta} \tag{44}$$

where $M = 100$.

To ensure that the integral constraint is satisfied through the period t_f, at every sampling time in which the LEMPC obtains the optimal control input trajectory, it utilizes the previously computed inputs u_1 to constrain the first step value of the control input trajectory u_1 at the current sampling time. Based on the cost function formulation, for maximization purposes, it is expected that C_A and T should be increased which results in the fact that at the beginning of the closed-loop simulation u_1 should rise to its maximum value and after a while it will go down to its lowest value to satisfy the integral constraint. We assume that the decrease of the Lyapunov function starts from the beginning of the simulation (i.e., $t' = 0$) for part of the system state (i.e., temperature). To maximize the production rate, we pick a temperature set-point near the boundary of the stability region ($T = 430$ K), considering the constraints on the control input
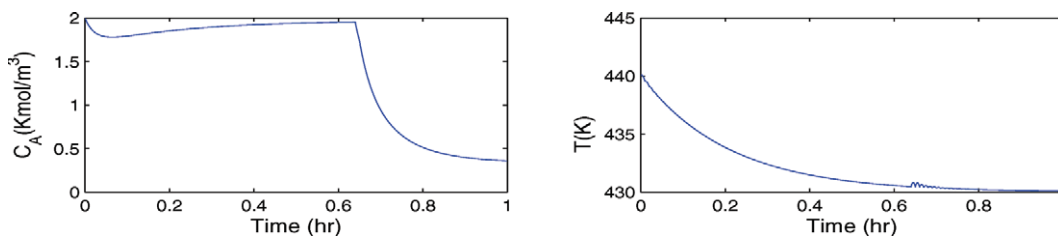
Figure 1. State trajectories of the process under the LEMPC design of Eq. 45 for initial condition $(C_A(0), T(0)) = (2\frac{kmol}{m^3}, 440K)$ without disturbances.

[Color figure can be viewed in the online issue, which is available at wileyonlinelibrary.com.]

Q. Due to the fact that the first differential equation (C_A) in Eq. 41 is input-to-state-stable (ISS) with respect to T, and the contractive constraint of Eq. 45g (see Eq. 45) ensures that the temperature converges to the set-point, the stability of the closed-loop system is guaranteed in the operating range of interest. To this end, we define $V_T(t_k) = (T(t_k) - 430)^2$. The LEMPC formulation for the chemical process example in question has the following form

$$\max_{u_1, u_2 \in S(\Delta)} \frac{1}{N\Delta} \int_{t_k}^{t_{k+N}} [k_0 e^{-\frac{E}{RT(\tau)}} C_A^2(\tau)] d\tau \tag{45a}$$

$$\dot{\tilde{x}}(t) = f(\tilde{x}(t)) + \sum_{i=1}^{2} g_i(\tilde{x}(t)) u_i(t) \tag{45b}$$

$$u_1(t) \in g_\zeta, \ \forall \ t \in [t_k, t_{k+1}) \tag{45c}$$

$$\tilde{x}(t_k) = x(t_k) \tag{45d}$$

$$\tilde{x}(t) \in \Omega_{\hat{\rho}} \tag{45e}$$

$$u_i(t) \in U_i \tag{45f}$$

$$\frac{dV_T(t_k)}{dT} (f_2(x(t_k)) + g_{22}(x(t_k)) u_2(t_k)) \leq -\gamma V_T(t_k) \tag{45g}$$

where $x(t_k)$ is the measurement of the process state at sampling time t_k, $\gamma = 9.53$ and the constraint of Eq. 45c implies that the first step value of u_1 should be chosen to satisfy the integral constraint where the explicit expression of g_ζ can be computed based on Eq. 44 and the magnitude constraint on u_1. Also, the constraint of Eq. 45g enforces the Lyapunov function, based on the temperature, to decrease from the beginning of the simulation. The simulations were carried out using Java programming language in a Pentium 3.20 GHz computer. The optimization problems were solved using the open source interior point optimizer Ipopt.[30]
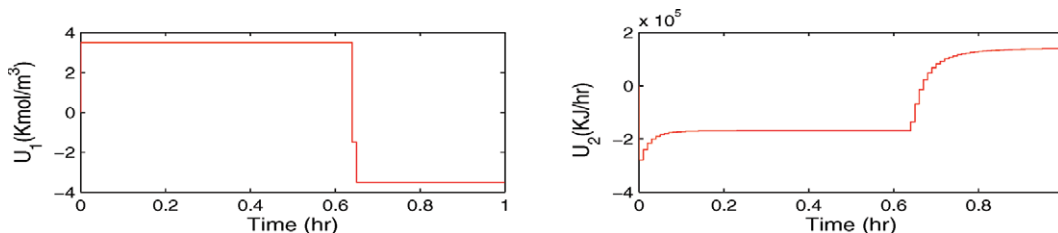
The purpose of the following set of simulations is to demonstrate that: (1) the proposed LEMPC design stabilizes the closed-loop system for different initial conditions; (2) the proposed LEMPC design maximizes the economic measure $L(x, u_1, u_2)$; (3) the proposed LEMPC design achieves practical closed-loop stability under different initial conditions; and (4) the proposed LEMPC design affords a higher cost function value compared to the steady-state operation. We consider two different scenarios in terms of the existence of process disturbance.

Figures 1 and 2 depict the state and manipulated input profiles, respectively, without process disturbances starting from the initial condition $(2\frac{kmol}{m^3}, 440K)$. Figures 3 and 4 depict the state and manipulated input profiles, respectively, without process disturbances starting from the initial condition $(2\frac{kmol}{m^3}, 400K)$. These simulations demonstrate that in the absence of disturbances the LEMPC of Eq. 45 drives the closed-loop system temperature at the desired steady-state, 430 K. Figures 5–8 show the corresponding state and manipulated input profiles starting from the two initial conditions under bounded process disturbances (Gaussian white noise with variances $\sigma_1 = 1$ kmol/m^3 and $\sigma_2 = 40$ K) with $|w_1| \leq 1$ kmol/m^3 and $|w_2| \leq 40$ K. Figure 9 shows a possible realization of the process disturbance. As expected, in all scenarios, u_1 goes up to its allowable maximum value to increase reactant concentration as much as possible early on (given the second-order reaction rate) and after a while it drops to its minimum value to satisfy the integral constraint ($\frac{1}{t_f} \int_0^{t_f} u_1(\tau) d\tau = 1$). On the other hand, the temperature rises as fast as possible when the temperature initial condition is below 430 K to maximize the reaction rate, and it decreases as slow as possible when the initial temperature is above 430 K to maintain the maximum possible reaction rate while satisfying the stability constraint; in both cases, the temperature finally settles at $T = 430$ K and the LEMPC design of Eq. 45 achieves practical stability. Figure 10 shows Ω_ρ with $\rho = 1405$ and three closed-loop system trajectories which

Figure 2. Manipulated input trajectories under the LEMPC design of Eq. 45 for initial condition $(C_A(0), T(0)) = (2\frac{kmol}{m^3}, 440K)$ without disturbances.

[Color figure can be viewed in the online issue, which is available at wileyonlinelibrary.com.]
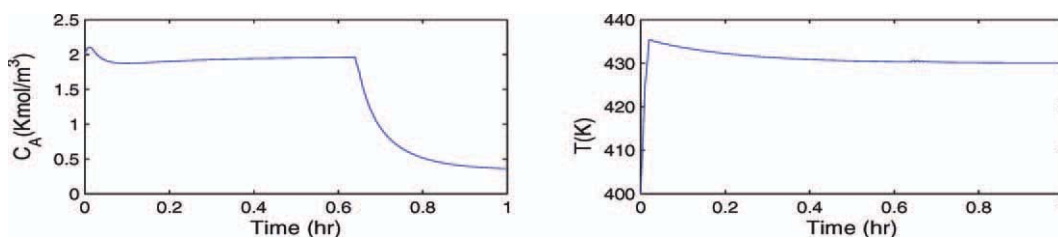
Figure 3. State trajectories of the process under the LEMPC design of Eq. 45 for initial condition $(C_A(0), T(0)) = (2 \frac{\text{kmol}}{\text{m}^3}, 400\text{K})$ without disturbances.
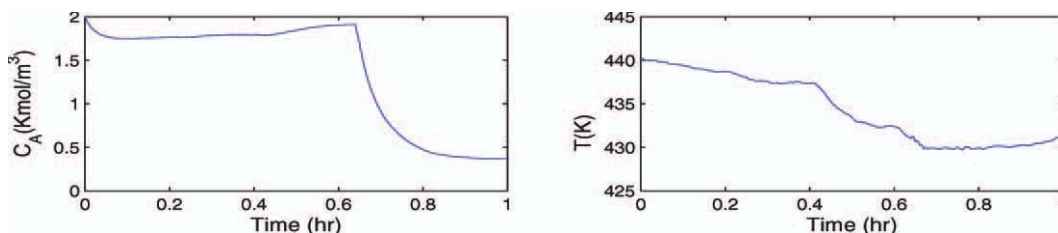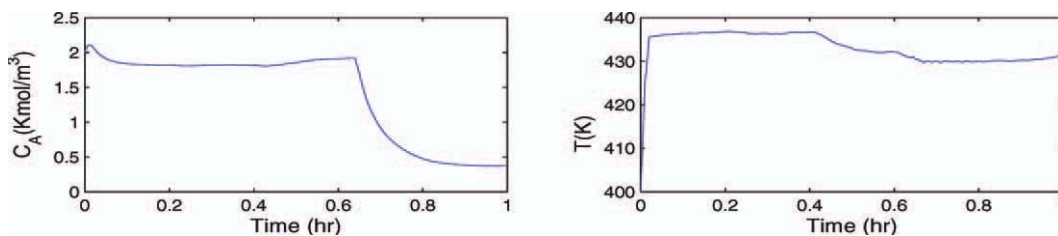
[Color figure can be viewed in the online issue, which is available at wileyonlinelibrary.com.]
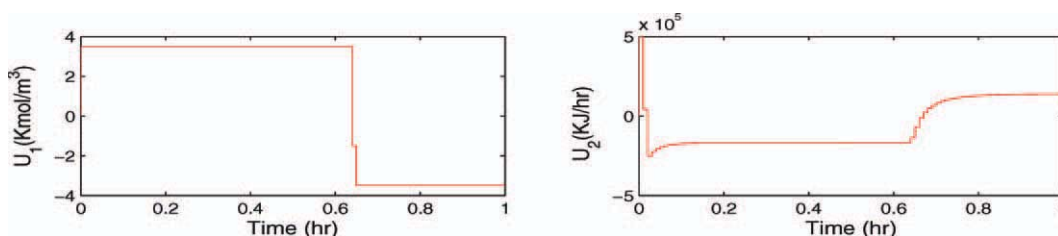
Figure 4. Manipulated input trajectories under the LEMPC design of Eq. 45 for initial condition $(C_A(0), T(0)) = (2 \frac{\text{kmol}}{\text{m}^3}, 400\text{K})$ without disturbances.

[Color figure can be viewed in the online issue, which is available at wileyonlinelibrary.com.]

start at $(2 \frac{\text{kmol}}{\text{m}^3}, 400\text{K})$ (inside of Ω_ρ; solid line), $(2 \frac{\text{kmol}}{\text{m}^3}, 440K)$ (inside of Ω_ρ; dotted line) and $(1 \frac{\text{kmol}}{\text{m}^3}, 500K)$ (outside of Ω_ρ; dashed line), respectively. This set of simulations demonstrates that in this case it is possible to achieve closed-loop stability even for initial conditions outside Ω_ρ, demonstrating that in the present example the computed Ω_ρ estimate is a rather conservative one.

Also, we have carried out a set of simulations to confirm that the application of the LEMPC design with the integral constraint on u_1 improves the economic objective function compared to the case that the system operates at

a steady-state satisfying the integral constraint. It should be mentioned that this comparison is performed under the case that there is no process disturbance. This steady-state is computed by assuming that the reactant material amount is equally distributed in the interval $[0,t_f]$. To carry out this comparison, we have computed the total cost of each scenario based on the index of the following form

$$J = \frac{1}{t_M} \sum_{i=0}^{M} [k_0 e^{-\frac{E}{RT(t_i)}} C_A^2(t_i)]$$

Figure 5. State trajectories of the process under the LEMPC design of Eq. 45 for initial condition $(C_A(0), T(0)) = (2 \frac{\text{kmol}}{\text{m}^3}, 440\text{K})$ subject to disturbances.

[Color figure can be viewed in the online issue, which is available at wileyonlinelibrary.com.]
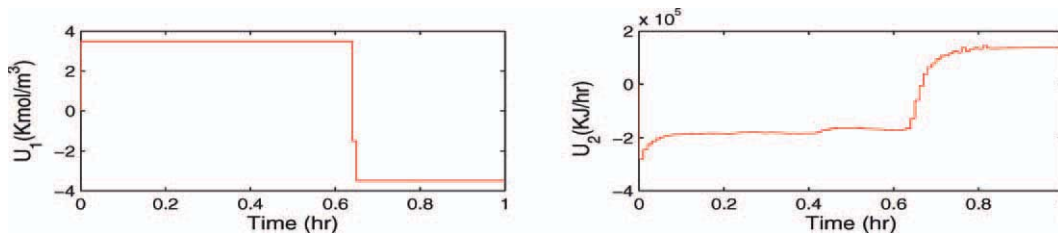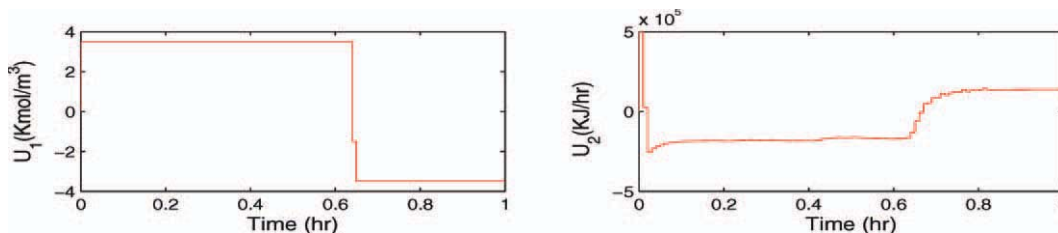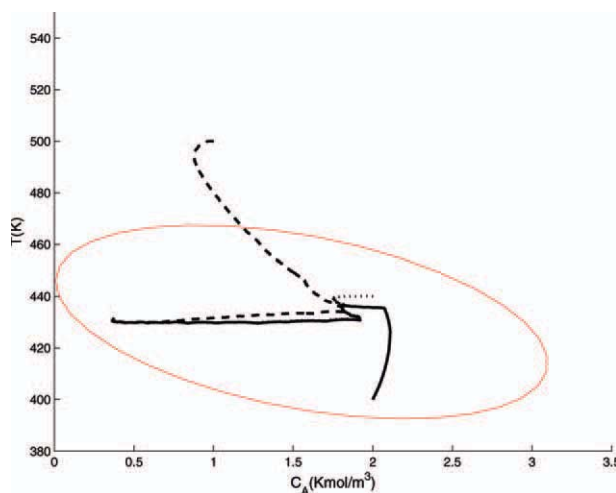

Figure 6. Manipulated input trajectories under the LEMPC design of Eq. 45 for initial condition $(C_A(0), T(0)) = (2 \frac{\text{kmol}}{\text{m}^3}, 440\text{K})$ subject to disturbances.

[Color figure can be viewed in the online issue, which is available at wileyonlinelibrary.com.]

Figure 7. State trajectories of the process under the LEMPC design of Eq. 45 for initial condition $(C_A(0), T(0)) = (2\frac{kmol}{m^3}, 400K)$ subject to disturbances.

[Color figure can be viewed in the online issue, which is available at wileyonlinelibrary.com.]

Figure 8. Manipulated input trajectories under the LEMPC design of Eq. 45 for initial condition $(C_A(0), T(0)) = (2\frac{kmol}{m^3}, 400K)$ subject to disturbances.

[Color figure can be viewed in the online issue, which is available at wileyonlinelibrary.com.]
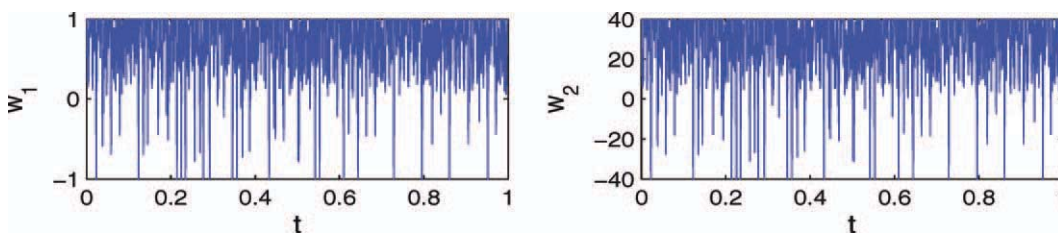
Figure 9. Disturbance realization for $\sigma_1 = 1$ kmol/m³ and $\sigma_2 = 40$ K with $|w_1| \leq 1$ kmol/m³ and $|w_2| \leq 40$ K.

[Color figure can be viewed in the online issue, which is available at wileyonlinelibrary.com.]

where $t_0 = 0$ hr, $t_M = 1$ hr, and $M = 100$. To be consistent in comparison we set u_1 to a constant value over the simulation such that it satisfies the integral constraint while letting u_2 be computed by the controller. By comparing the cost function values, we find that in the proposed LEMPC design via time-varying operation (starting from $(C_A, T) = (2\frac{kmol}{m^3}, 400K)$), the cost function achieves a higher value (19299.47) compared to the case of steady-state operation (17722.07) (i.e., equal in time distribution of the reactant). Also, by starting from $(C_A, T) = (2\frac{kmol}{m^3}, 440K)$, the cost function achieves a higher value (19459.67) compared to the case of steady-state operation (17852.85).

Asynchronous measurements with delay

For this set of simulations, it is assumed that the state measurements of the process are available asynchronously at time instants $\{t_{a \geq 0}\}$ with an upper bound $T_m = 6\Delta$ on the maximum interval between two successive asynchronous state measurements, where Δ is the controller and sensor sampling time and is chosen to be $\Delta = 0.01$ hr $= 36$ sec. To model the time sequence $\{t_{a \geq 0}\}$, we use an upper bounded Poisson process. The Poisson process is defined by the number of events

Figure 10. Estimation of Ω_ρ and three closed-loop system trajectories for synchronous measurement case with disturbances.

[Color figure can be viewed in the online issue, which is available at wileyonlinelibrary.com.]
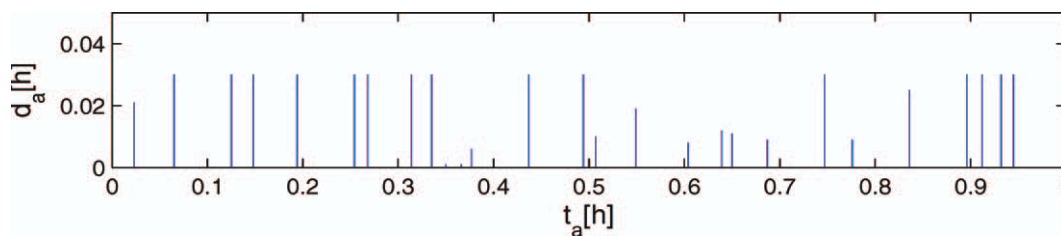
Figure 11. Asynchronous measurement sampling times and their associated delay.

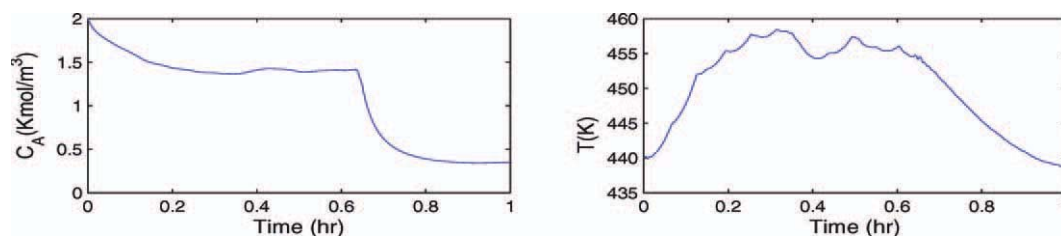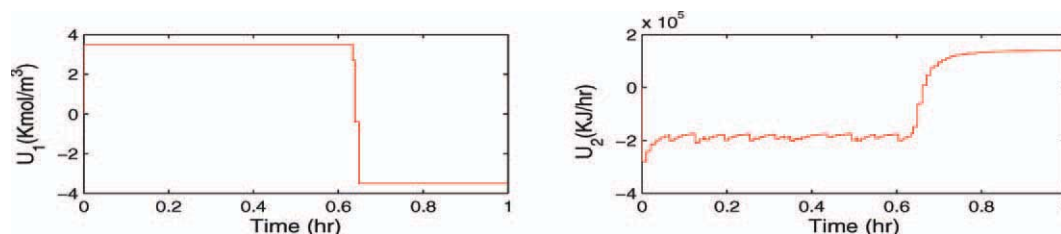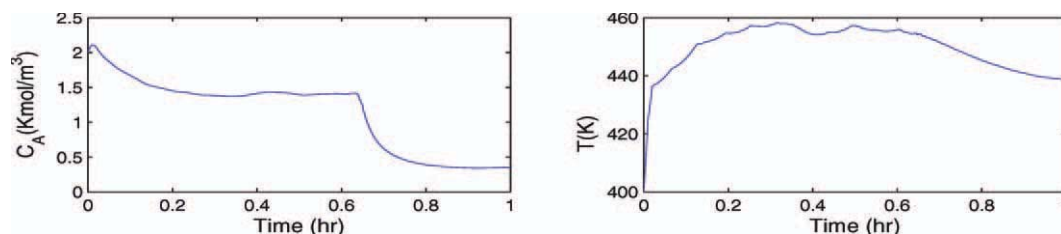[Color figure can be viewed in the online issue, which is available at wileyonlinelibrary.com.]

Figure 12. State trajectories of the process under the LEMPC design of Eq. 46 for initial condition $(C_A(0), T(0)) = (2\frac{kmol}{m^3}, 440K)$ subject to asynchronous and delayed measurements and disturbances.

[Color figure can be viewed in the online issue, which is available at wileyonlinelibrary.com.]

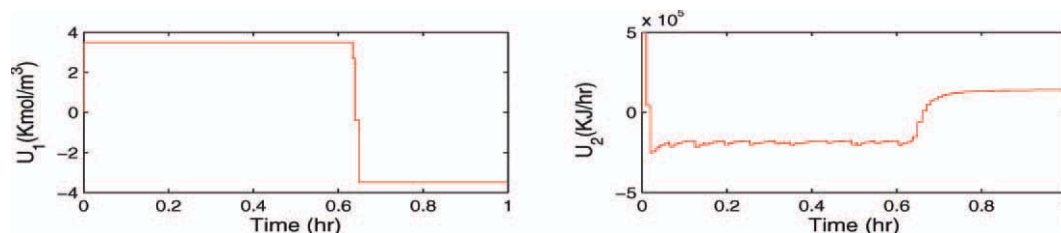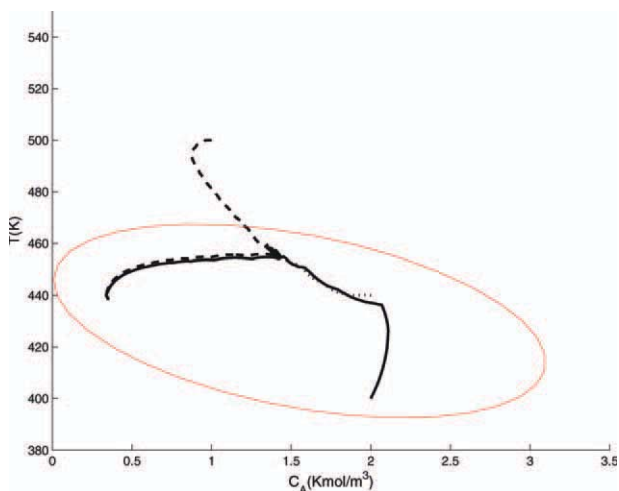**Figure 13. Manipulated input trajectories under the LEMPC design of Eq. 46 for initial condition $(C_A(0), T(0)) = (2\frac{kmol}{m^3}, 440K)$ subject to asynchronous and delayed measurements and disturbances.**

[Color figure can be viewed in the online issue, which is available at wileyonlinelibrary.com.]

Figure 14. State trajectories of the process under the LEMPC design of Eq. 46 for initial condition $(C_A(0), T(0)) = (2\frac{kmol}{m^3}, 400K)$ subject to asynchronous and delayed measurements and disturbances.

[Color figure can be viewed in the online issue, which is available at wileyonlinelibrary.com.]

Figure 15. Manipulated input trajectories under the LEMPC design of Eq. 46 for initial condition $(C_A(0), T(0)) = (2\frac{kmol}{m^3}, 400K)$ subject to asynchronous and delayed measurements and disturbances.
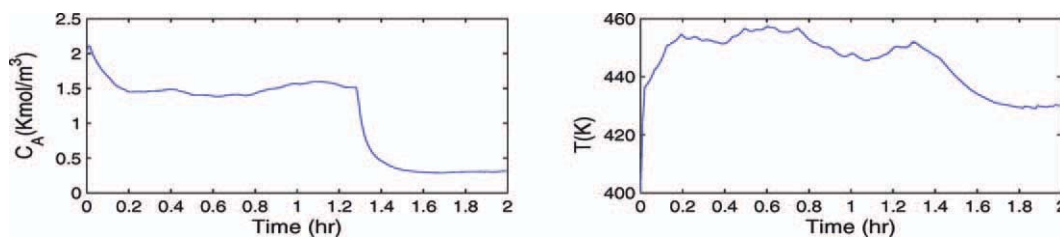
[Color figure can be viewed in the online issue, which is available at wileyonlinelibrary.com.]

per unit time W. The interval between two successive concentration sampling times (events of the Poisson process) is given by $\Delta_a = \min\{-ln\chi/W, T_m\}$, where χ is a random variable with uniform probability distribution between 0 and 1. This generation ensures that $\max_a\{t_{a+1} - t_a\} \leq T_m$. In this example, W is chosen to be $W = 25$. A Gaussian random process is used to generate the associated delay sequence $\{d_{a\geq0}\}$ with $d_a \leq D$ while $D = 3\Delta$. Figure 11 shows the asynchronous time instants when measurements are available and the corresponding delay size associated with each measurement.


Figure 16. Estimation of Ω_ρ and three closed-loop system trajectories for asynchronous measurement case with disturbances.

[Color figure can be viewed in the online issue, which is available at wileyonlinelibrary.com.]

The LEMPC formulation for the chemical process example in question subject to asynchronous and delayed state measurements has the following form

$$\max_{u_1,u_2\in S(\Delta)} \frac{1}{N\Delta} \int_{t_a}^{t_a+N\Delta} [k_0 e^{-\frac{E}{RT(\tau)}}C_A^2(\tau)]d\tau \quad (46a)$$

$$\dot{\check{x}}(t) = f(\check{x}(t)) + \sum_{i=1}^{2} g_i(\check{x}(t))u_i^*(t), \; \forall \, t \in [t_a - d_a, t_a) \quad (46b)$$

$$\dot{\check{x}}(t) = f(\check{x}(t)) + \sum_{i=1}^{2} g_i(\check{x}(t))u_i(t), \; \forall \, t \in [t_a, t_a + N\Delta) \quad (46c)$$

$$u_1(t) \in g_\zeta, \; \forall \, t \in [t_a, t_a + N\Delta) \quad (46d)$$

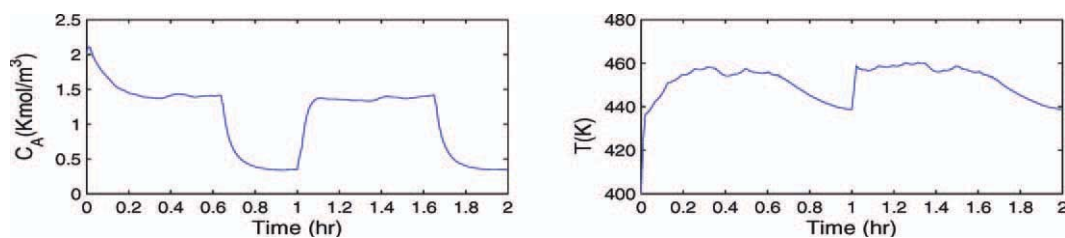$$\check{x}(t_a - d_a) = x(t_a - d_a) \quad (46e)$$

$$\check{x}(t) \in \Omega_{\hat{\rho}} \quad (46f)$$

$$u_i(t) \in U_i \quad (46g)$$

$$V_T(t_a + (l+1)\Delta) \leq \beta V_T(t_a + l\Delta) \; l = 0, ..., N_{Da} \quad (46h)$$

where $x(t_a)$ is the measurement of the process state at sampling time t_a and $\beta = 1/1.1 = 0.909$. The constraint of Eq. 46h forces the Lyapunov function, based on the temperature, to decrease for N_{Da} sampling times.

Figures 12 and 13 show the state and manipulated input profiles, respectively, starting from the initial condition $(2\frac{kmol}{m^3}, 440K)$ under bounded process disturbances (the same to the ones used in the case of synchronous measurement sampling). Figures 14 and 15 show the corresponding state and manipulated input profiles, respectively, starting from the initial condition $(2\frac{kmol}{m^3}, 400K)$, respectively. From these

Figure 17. State trajectories of the process under the LEMPC design of Eq. 46 for initial condition $(C_A(0), T(0)) = (2\frac{kmol}{m^3}, 400K)$ subject to asynchronous and delayed measurements and disturbances under enforcing the integral constraint over a two-hour period.

[Color figure can be viewed in the online issue, which is available at wileyonlinelibrary.com.]
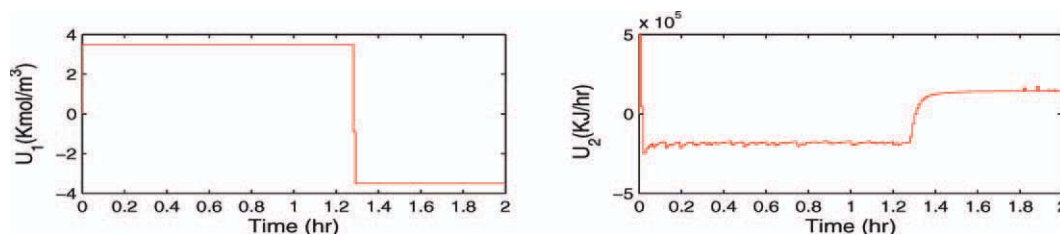
Figure 18. Manipulated input trajectories under the LEMPC design of Eq. 46 for initial condition $(C_A(0), T(0)) = (2\frac{kmol}{m^3}, 400K)$ subject to asynchronous and delayed measurements and disturbances under enforcing the integral constraint over a two-hour period.

[Color figure can be viewed in the online issue, which is available at wileyonlinelibrary.com.]

Figure 19. State trajectories of the process under the LEMPC design of Eq. 46 for initial condition $(C_A(0), T(0)) = (2\frac{kmol}{m^3}, 400K)$ subject to asynchronous and delayed measurements and disturbances under enforcing the integral constraint over two consecutive one-hour periods.

[Color figure can be viewed in the online issue, which is available at wileyonlinelibrary.com.]
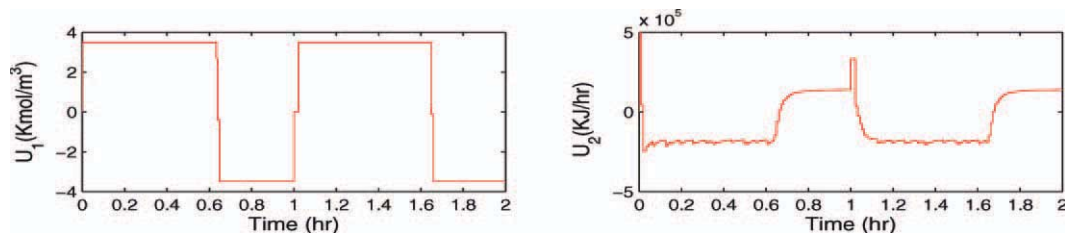
Figure 20. Manipulated input trajectories under the LEMPC design of Eq. 46 for initial condition $(C_A(0), T(0)) = (2\frac{kmol}{m^3}, 400K)$ subject to asynchronous and delayed measurements and disturbances under enforcing the integral constraint over two consecutive one-hour periods.

[Color figure can be viewed in the online issue, which is available at wileyonlinelibrary.com.]

figures, we can see similar results as in the case of synchronous measurement sampling, such as, u_1 goes up to its allowable maximum value to increase the reactant concentration as much as possible early on and the temperature rises as fast as possible when the temperature initial condition is below 430 K to maximize the reaction rate and it decreases as slow as possible when the initial temperature is above 430 K to maintain the maximum possible reaction rate. From these figures, we can also see that the practical stability of the closed-loop system is ensured in the presence of asynchronous and delayed measurements. This is because in the design of the LEMPC of Eq. 46, asynchronous and delayed measurements are taken explicitly into account. Similar to the synchronous measurement case, Figure 16 shows Ω_ρ with $\rho = 1405$ and three closed-loop system trajectories which start at $(2\frac{kmol}{m^3}, 400K)$ (inside of Ω_ρ; solid line), $(2\frac{kmol}{m^3}, 440K)$ (inside of Ω_ρ; dotted line) and $(1\frac{kmol}{m^3}, 500K)$ (outside of Ω_ρ; dashed line), respectively.

Finally, we have also carried out two sets of simulations in which: (a) the integral constraint is enforced over a time period of two hours and (b) the integral constraint is enforced over two consecutive one-hour periods. Figures 17 and 18 depict the state and input trajectories of the closed-loop system in case (a) and Figures 19 and 20 depict the state and input trajectories in case (b). These figures illustrate that the periodic operation of the plant under the proposed LEMPC can be readily achieved for different operating scenarios.

Conclusions

In this work, we developed LEMPC designs which are capable of optimizing closed-loop performance with respect to general economic considerations for nonlinear systems.

First, we considered nonlinear systems with synchronous measurement sampling and uncertain variables, and designed an LEMPC via Lyapunov-based techniques. The proposed LEMPC design has two different operation modes. The first operation mode corresponds to the period in which the cost function should be optimized; and in this operation mode, the LEMPC maintains the closed-loop system state within the stability region and optimizes the cost function to its maximum extent. The second operation mode corresponds to operation in which the system is driven by the LEMPC to an appropriate steady-state. Subsequently, we extended the results to nonlinear systems subject to asynchronous and delayed measurements and uncertain variables. In both LEMPC designs, suitable constraints were incorporated to guarantee that the closed-loop system state is always bounded in the stability region and is ultimately bounded in small regions containing the origin. The theoretical results were illustrated through a chemical process example.

Literature Cited

1. Marlin TE, Hrymak AN. Real-time operations optimization of continuous processes. *AIChE Symp Ser CPC V*. 1997;93:156–164.
2. García CE, Prett DM, Morari M. Model predictive control: theory and practice–a survey. *Automatica*. 1989;25:335–348.
3. Mayne DQ, Rawlings JB, Rao CV, Scokaert POM. Constrained model predictive control: stability and optimality. *Automatica*. 2000; 36:789–814.

4. Backx T, Bosgra O, Marquardt W. Integration of model predictive control and optimization of processes: enabling technology for market driven process operation. In: *Proceedings of the IFAC Symposium on Advanced Control of Chemical Processes*. Pisa, Italy, 2000: 249–260.

5. Rawlings JB, Amrit R. Optimizing process economic performance using model predictive control. In: Magni L, Raimondo DM, Allgöwer F. *Nonlinear Model Predictive Control, Lecture Notes in Control and Information Science Series*. Berlin: Springer, 2009: 119–138.

6. Kadam JV, Marquardt W. Integration of economical optimization and control for intentionally transient process operation. Assessment and future directions of nonlinear model predictive control. *Lect Notes Contr Inform Sci Ser*. 2007;358:419–434.

7. Brosilow C, Zhao GQ, Rao KC. A linear programming approach to constrained multivariable control. In: *Proceedings of the American Control Conference*. San Diego, CA, 1984:667–674.

8. Muske KR. Steady-state target optimization in linear model predictive control. In: *Proceedings of the American Control Conference*. Albuquerque, New Mexico, 1997:3597–3601.

9. Morshedi AM, Cutler CR, Skrovanek TA. Optimal solution of dynamic matrix control with linear programing techniques. In: *Proceedings of the American Control Conference*. Boston, MA, 1985:199–208.

10. Yousfi C, Tournier R. Steady state optimization inside model predictive control. In: *Proceedings of the American Control Conference*. Boston, MA, 1991:1866–1870.

11. de Gouvea MT, Odloak D. One-layer real time optimization of lpg production in the FCC unit: procedure, advantages and disadvantages. *Comput Chem Eng*. 1998;22:191–198.

12. Zanin AC, de Gouvea MT, Odloak D. Integrating real-time optimization into the model predictive controller of the FCC system. *Contr Eng Pract*. 2002;10:819–831.

13. Zhu X, Hong W, Wang S. Implementation of advanced control for a heat-integrated distillation column system. In: *Proceedings of the 30th Annual Conference of IEEE Industrial Electronics Society*. Busan, Korea, 2004:2006–2011.

14. Engell S. Feedback control for optimal process operation. *J Process Contr*. 2007;17:203–219.

15. Huang R, Harinath E, Biegler LT. Lyapunov stability of economically-oriented nmpc for cyclic processes. *J Process Contr*. 2011;21:501–509.

16. Diehl M, Amrit R, Rawlings JB. A Lyapunov function for economic optimizing model predictive control. *IEEE Trans Automat Contr*. In press.

17. Lin Y, Sontag ED, Wang Y. A smooth converse Lyapunov theorem for robust stability. *SIAM J Contr Optim*. 1996;34:124–160.

18. Christofides PD, El-Farra NH. *Control of Nonlinear and Hybrid Process Systems: Designs for Uncertainty, Constraints and Time-Delays*. Berlin, Germany: Springer-Verlag, 2005.

19. Kokotovic P, Arcak M. Constructive nonlinear control: a historical perspective. *Automatica*. 2001;37:637–662.

20. Lin Y, Sontag ED. A universal formula for stabilization with bounded controls. *Syst Control Lett*. 1991;16:393–397.

21. El-Farra NH, Christofides PD. Bounded robust control of constrained multivariable nonlinear processes. *Chem Eng Sci*. 2003;58: 3025–3047.

22. Mhaskar P, El-Farra NH, Christofides PD. Stabilization of nonlinear systems with state and control constraints using Lyapunov-based predictive control. *Syst Control Lett*. 2006;55:650–659.

23. Liu J, Chen X, Muñoz de la Peña D, Christofides PD. Sequential and iterative architectures for distributed model predictive control of nonlinear process systems. *AIChE J*. 2010;56:2137–2149.

24. Muñoz de la Peña D, Christofides PD. Lyapunov-based model predictive control of nonlinear systems subject to data losses. *IEEE Trans Automatic Control*. 2008;53:2076–2089.

25. Liu J, Muñoz de la Peña D, Christofides PD, Davis JF. Lyapunov-based model predictive control of nonlinear systems subject to time-varying measurement delays. *Int J Adaptive Control Signal Process*. 2009;23:788–807.

26. Lee C, Bailey J. Modification of consecutive-competitive reaction selectivity by periodic operation. *Ind Eng Chem Process Design Deve*. 1980;19:160–166.

27. Sincic D, Bailey J. Analytical optimization and sensitivity analysis of forced periodic chemical processes. *Chem Eng Sci*. 1980;35: 1153–1161.

28. Watanabe N, Onogi K, Matsubara M. Periodic control of continuous stirred tank reactors–I: the Pi criterion and its applications to isothermal cases. *Chem Eng Sci*. 1981;36:809–818.

29. Watanabe N, Kurimoto H, Matsubara M, Onogi K. Periodic control of continuous stirred tank reactors–II: cases of a nonisothermal single reactor. *Chem Eng Sci*. 1982;37:745–752.

30. Wächter A, Biegler LT. On the implementation of primal-dual interior point filter line search algorithm for large-scale nonlinear programming. *Math Program*. 2006;106:25–57.